

RESIDUAL STRESS ANALYSIS IN
THICK-WALLED CIRCULAR CYLINDERS

A THESIS

Presented to

The Faculty of the Division of Graduate
Studies and Research

By

Calvin Runkle Jameson

In Partial Fulfillment

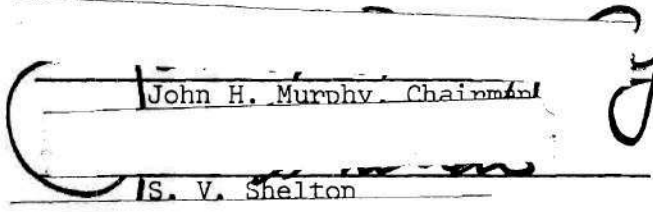
of the Requirements for the Degree
Master of Science in Mechanical Engineering

Georgia Institute of Technology

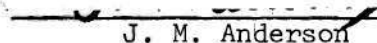
September, 1973

RESIDUAL STRESS ANALYSIS IN
THICK-WALLED CIRCULAR CYLINDERS

Approved:

_____
John H. Murphy, Chairman

_____
S. V. Shelton

_____
J. M. Anderson

Date approved by Chairman: 6/13/73

TABLE OF CONTENTS

	Page
LIST OF TABLES	ii
LIST OF ILLUSTRATIONS.	iii
NOMENCLATURE	iv
SUMMARY.	vi
Chapter	
I. INTRODUCTION.	1
II. BASIC ANALYTICAL AND EXPERIMENTAL METHODS	9
Elastic Deformation of a Cylinder	
Elastic Solution for a Cylinder with Internal Pressure	
Yield Conditions	
Plastic Deformation of a Cylinder	
Hoffman-Sachs Solution	
Coffin-MacGregor Partially Plastic Solution	
Thermal Stress Analysis	
Mendelson and Manson Procedure	
Experimental Determination	
Sachs Boring Out Method	
III. ANALYTICAL RESULTS.	37
Variable Properties	
Residual Autofrettage Stresses	
Machining	
Thermal Stresses	
Final Residual Stresses Distribution	
Bore Diameter	
IV. EXPERIMENTAL RESULTS.	47
V. DISCUSSION.	53
APPENDIX	61
BIBLIOGRAPHY	64

LIST OF TABLES

Table		Page
1.	Bore Diameter Measurements Across Grooves Before and After 2245.62 Equivalent Service Rounds	56
2.	Calculation Procedure for Experimental Residual Stresses. .	57
3.	Elastic Thermal Stresses.	59
4.	Action Autofrettage Stresses.	60

LIST OF ILLUSTRATIONS

Figure	Page
1. Gun and Test Sections	3
2. Temperature Distribution in Hollow Cylinders.	6
3. A Cross Section of the Bore	10
4. Stress Element in Polar Coordinates	11
5. Deformation in Polar Coordinates.	11
6. Residual Autofrettage Radial Stresses	40
7. Residual Autofrettage Tangential Stresses	41
8. Residual Autofrettage Axial Stresses.	42
9. Residual Thermal Radial Stress.	50
10. Residual Thermal Tangential Stress.	51
11. Residual Thermal Axial Stress	52

NOMENCLATURE

a	inside radius
b	outside radius
E	elastic modulus
e	strain
P	pressure
r	radial distance
S	stress
T	temperature
u	radial displacement
α	coefficient of thermal expansion
ϵ	strain
ν	Poisson's ratio
σ	stress

Subscripts:

a	inside radius
b	outside radius
e	equivalent
ep	equivalent plastic
et	equivalent total
i	inside surface
n	n^{th} point

o	outside surface
p	plastic
r	radial
t	tangential
z	longitudinal
θ	tangential
τ	shear stress
ρ	radius of elastic-plastic interface

SUMMARY

A problem encountered in some large thick-walled cylinders, gun barrels, is the decrease in bore diameter after some period of sustained use. The stress history of these guns consists of initial pre-stressing (autofrettage) followed by the pressure and thermal stresses resulting from rapid firing.

Experimental data for a five-inch naval gun are available. These data consist of the final existing strain measurements. It is the object of this investigation to determine if the final stress state can be correctly predicted by analytical calculations.

Analytical calculations included elastic and plastic material behavior as well as temperature-dependent mechanical properties. The numerical method developed by Mendelson and Manson was used. The solution developed agreed with the experimental data from the inner surface to halfway along the radius of the cylinder.

CHAPTER I

INTRODUCTION

The objective of this thesis is to predict the final state of stress and strain existing in a thick-walled tube which has been subjected to a large internal pressure followed by a thermal stressing due to heating. This problem is associated with the loading history of the barrel of certain large guns. A typical loading history for a large gun barrel consists of first applying an internal pressure which severely cold works the material at the inner bore and results in residual compressive stresses upon removal of the pressure. This process is referred to as autofrettage. After autofrettage, some machining of the inner bore may be necessary in order to restore the proper bore diameter. When the gun is then used in a rapid fire condition, a temperature gradient develops in the gun barrel resulting in thermal stresses.

A problem which may develop is the permanent decrease in the diameter of the bore after the rapid fire condition. A particular example of this was encountered in a five-inch naval gun and a project was established at the Massachusetts Institute of Technology (M.I.T.)^{*} to analyze the problem (8).

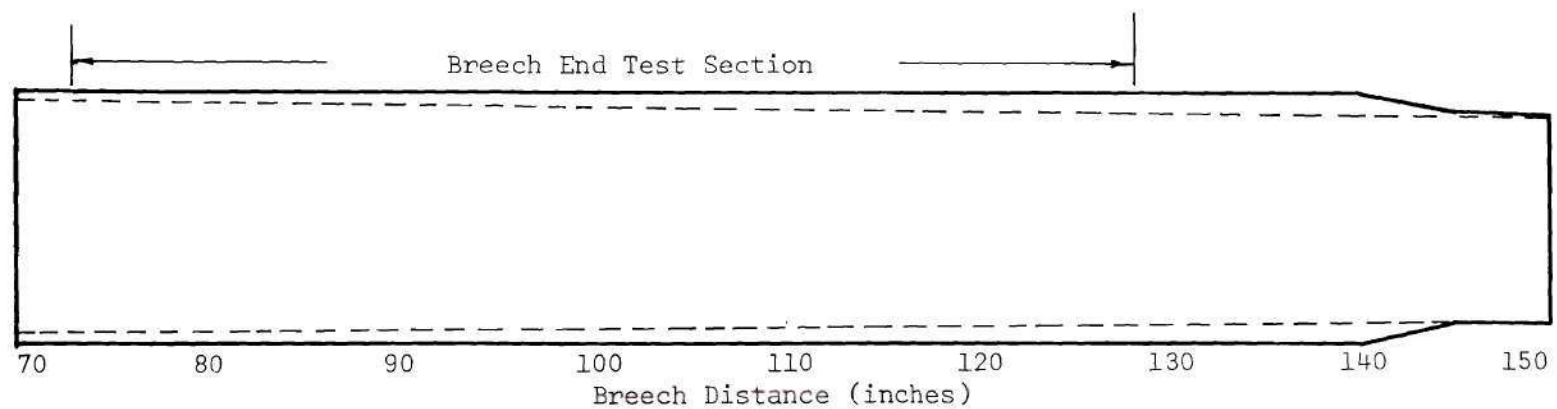
The M.I.T. project was provided two approximately three-foot

^{*}The work at M.I.T. was conducted by the late Dr. W. R. Clough, who suggested and initiated the extension presented in this thesis.

sections of a five-inch gun. The gun from which the sections were cut had been subjected to 2245.62 equivalent service rounds and was one in which a permanent bore diameter decrease had been encountered. One of the three-foot lengths was that which terminated in the muzzle; the other extended from 73 inches to 128.5 inches from the breech (see Figure 1).

The muzzle end was small enough to allow residual stress determination at M.I.T. by the Sachs boring out or turning down method. This method developed by G. Sachs for cylinders, rods and thick-walled tubes accounts for all three principal stresses and only assumes rotational symmetry about the axis of the tube and no change along its length. The method itself consists of boring out or turning down the tube in steps and measuring the dimensional change of the tube. For accuracy the length of the tube should be several times the diameter. The larger section was forwarded to the Naval Gun Factory as it was too large to be machined at the M.I.T. Machine Tool Laboratory. Data for this section were not available at the time the project was disbanded.

A preliminary review, at M.I.T., of the circumstances surrounding the bore diameter decrease led to the conclusion that this was the result of the combined effects of the radial expansion residual stresses and the high gun temperatures which give rise to thermal stresses of a large order of magnitude. The temperature at the surface of the bore has been estimated to be about 365°C after firing (8). The Bureau of Ordnance calculations indicate that the residual autofrettage stresses at the bore at 77,985 psi in compression in the tangential or hoop



--- Dimensions of Machined Gun Barrel

— Dimensions of Original Forging

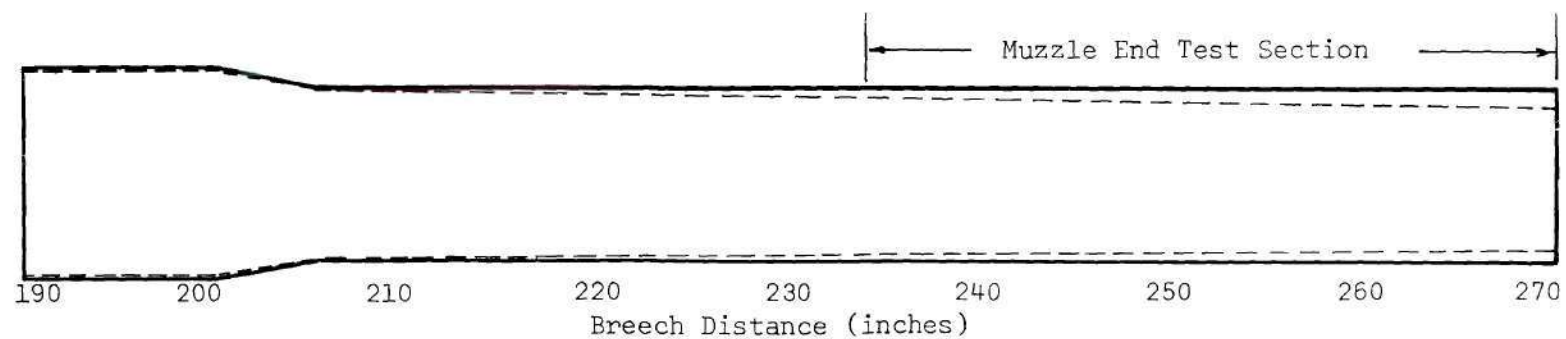


Figure 1. Gun and Test Sections

direction. If elastic thermal stresses due to a 300°C temperature differential and a logarithmic distribution are superimposed on the autofrettage stress a compressive stress of 167,715 psi results. A stress of such magnitude would in all likelihood cause compressive yielding and explain the bore decrease. Only qualitative results were possible from the M.I.T. study because the thermal stress analysis did not include plastic strain or temperature-dependent properties.

In this thesis the analysis of the final stress state and subsequent bore diameter decrease is extended to include a plasticity solution for the thermal stresses which incorporates the variance of properties with temperature. In order to include the plastic strain and temperature-dependent properties it is necessary to use a numerical solution. The best method seems to be the iterative solution developed by A. Mendelson and S. S. Manson (5).

The method of analysis of the final residual stress state is as follows:

1. The calculation of the rest or residual autofrettage stresses. To carry out this, it is first necessary to calculate the action stresses present when a high liquid internal pressure is applied. This solution is arrived at from plasticity theory since the magnitude of the internal pressure is sufficient to cause considerable plastic deformation. The second step is to calculate the stresses caused by the internal pressure using purely elastic theory. By subtracting the purely elastic solution from the plasticity theory solution the residual stresses can be obtained. This assumes no further reyielding.

2. A temperature distribution of some kind is necessary for the calculation of the thermal stresses. Since the gun barrel is inherently one of rotational symmetry it is satisfactory to assume a temperature distribution that is a function of radius only and does not vary along the length of the gun barrel. With each round fired there will be a temperature fluctuation and hence a transient state temperature distribution. However, it is judged that a gun fired at equal intervals in rapid fire could eventually be approximated as a steady state conduction problem. Therefore, for this analysis a steady state logarithmic distribution is assumed.

The equilibrium temperature distribution is

$$T(r) = T_i - \frac{T_i - T_o}{\ln(r_o/r_i)} \ln(r/r_i)$$

as shown in Figure 2.

Since thermal stresses arise from the difference in temperature along the cross section the lower temperature, in this case the outside, can be assumed to be zero in order to simplify the relationship.

Thus:

$$T(r) = \frac{\Delta T \ln(r_o/r)}{\ln(r_o/r_i)}$$

where $\Delta T = T_i - T_o$.

3. The calculation of the final residual stress and strains will be done as follows. It is necessary to use the method developed by

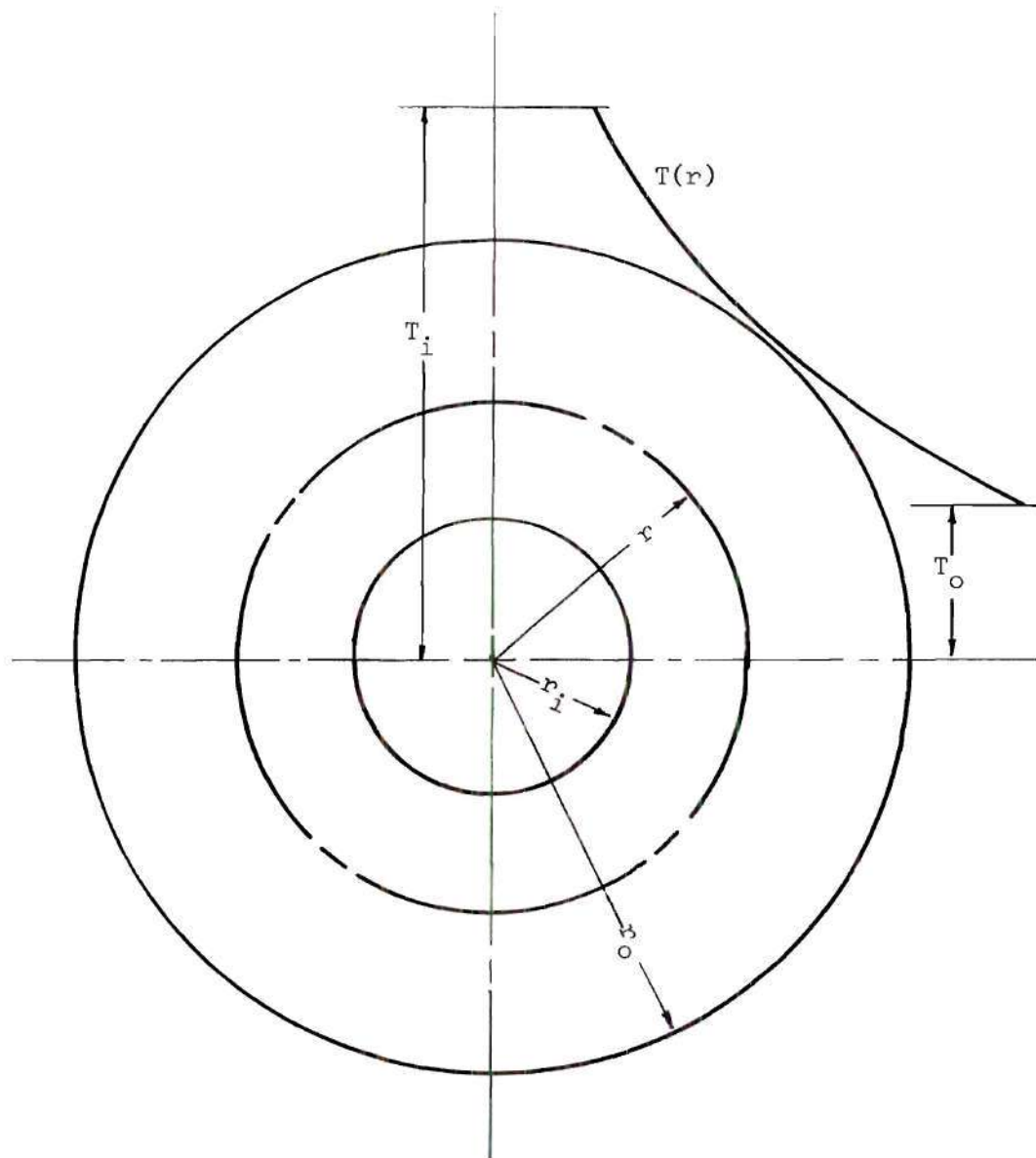


Figure 2. Temperature Distribution in a Hollow Cylinder

Mendelson and Manson which is basically an iterative numerical solution. First the state of strain caused by the autofrettage residual stresses is considered the permanent deformation of the cylinder at the time of application of the temperature distribution.

Using this plastic strain and logarithmic temperature distribution the thermal stresses are calculated. In several places the combined stresses will be above the yield point of the material causing further plastic flow. The thermal stresses are then recalculated with the further plastic deformation. This procedure is repeated until convergence to the action thermal stresses and total plastic deformation are obtained. Using this total plastic deformation the temperature is removed and the stresses recalculated. If any further yielding occurs the total plastic deformation is adjusted accordingly and the stresses adjusted correspondingly.

For the calculation of the thermal action stresses, the temperature variation of the yield strength, Young's modulus of elasticity and the coefficient of expansion were considered. Work hardening effects were ignored because in the ranges of plastic strain encountered the steel behaves as a perfectly plastic material.

Recall the autofrettage process induces compressive stress at the inner surface. The thermal gradient causes a further compressive stress. In fact, this further stress causes yielding of the material near the bore in compression. After the thermal load is removed this permanent compressive deformation causes a tensile residual tangential or hoop stress which in turn causes a decrease in bore diameter.

If a transient analysis was attempted the slope of the temperature curve would naturally be steeper. The area closer to the bore would be more highly stressed than in the steady state analysis. Consequently there will be more plastic deformation in the area near the bore and less further toward the outside than using a steady state analysis. There will be increased values of final residual stresses resulting from the larger amounts of plastic deformation.

CHAPTER II

BASIC ANALYTICAL AND EXPERIMENTAL METHODS

Elastic Deformation of a Cylinder

If a long circular cylinder of uniform thickness is subjected to a uniformly distributed internal pressure the deformation produced is symmetrical about the axis of the cylinder and does not vary along its length (2).

Consider a section cut from the cylinder perpendicular to the axis (see Figure 3).

From the condition of symmetry there are no shear forces and the displacements are radial. Since there are no shear stresses a stress element appears as in Figure 4.

By summing the forces in the radial (r) direction the equilibrium equation is developed.

$$\frac{d\sigma_r}{dr} + \frac{\sigma_r - \sigma_t}{r} = 0$$

Now consider the same ring from a displacement point of view remembering the condition of symmetry (see Figure 5). Engineering strain is defined as change of length divided by the original length.

$$\epsilon_r = \frac{\Delta L_r}{L_r} = \frac{u + \frac{du}{dr} dr - u}{dr} = \frac{du}{dr}$$

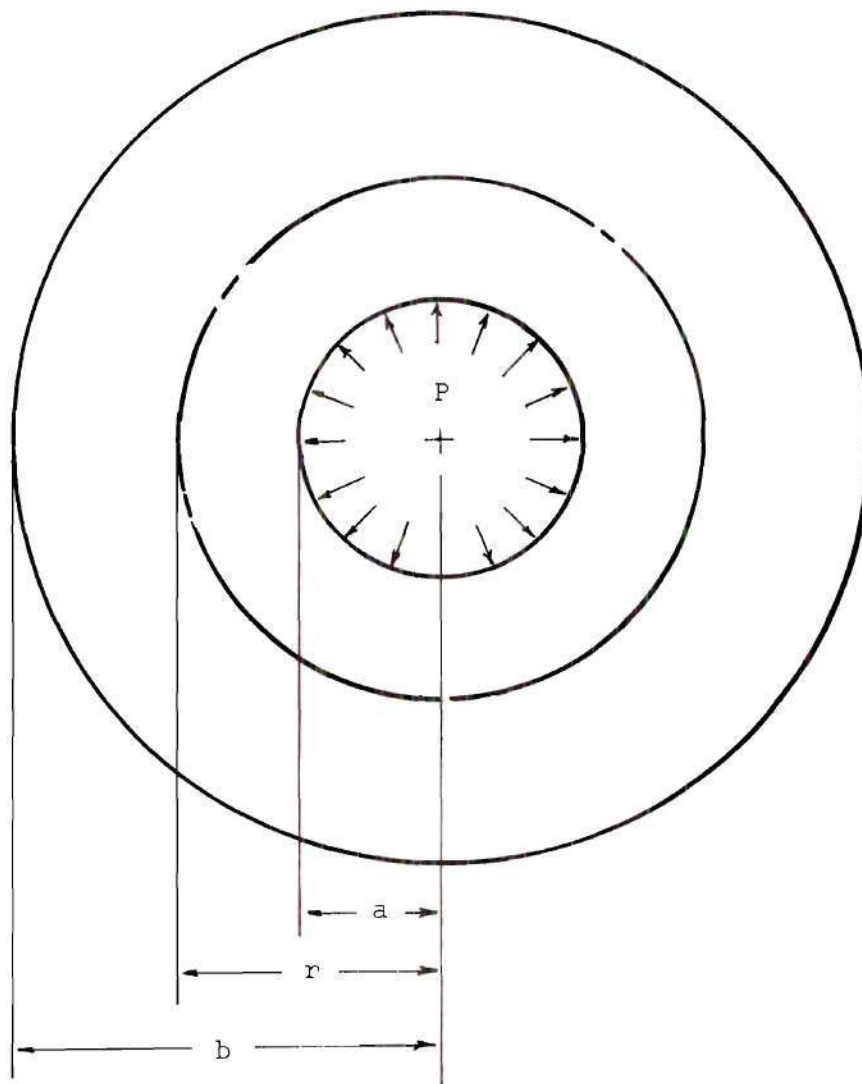


Figure 3. A Cross Section of the Bore

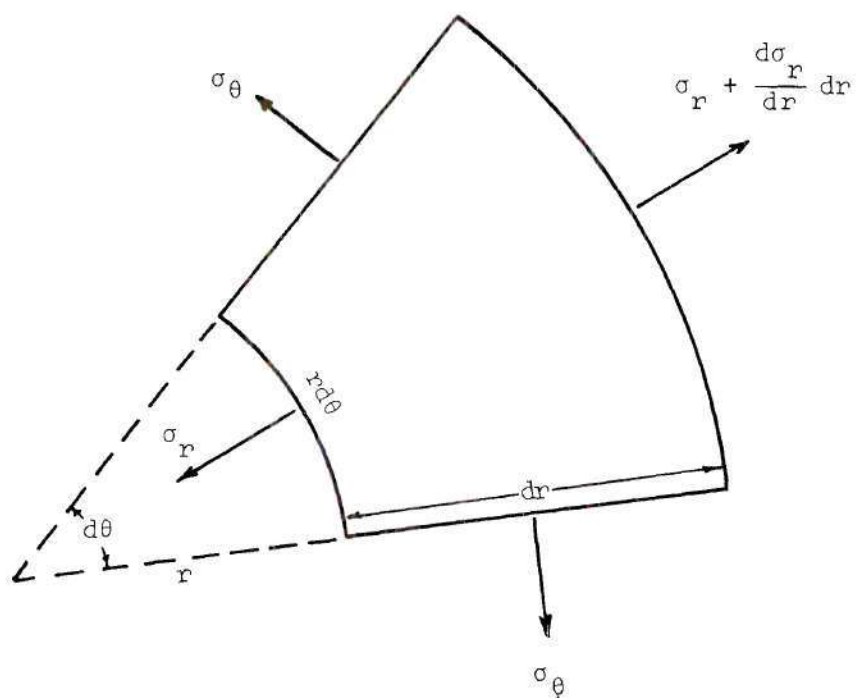


Figure 4. Stress Element in Polar Coordinates

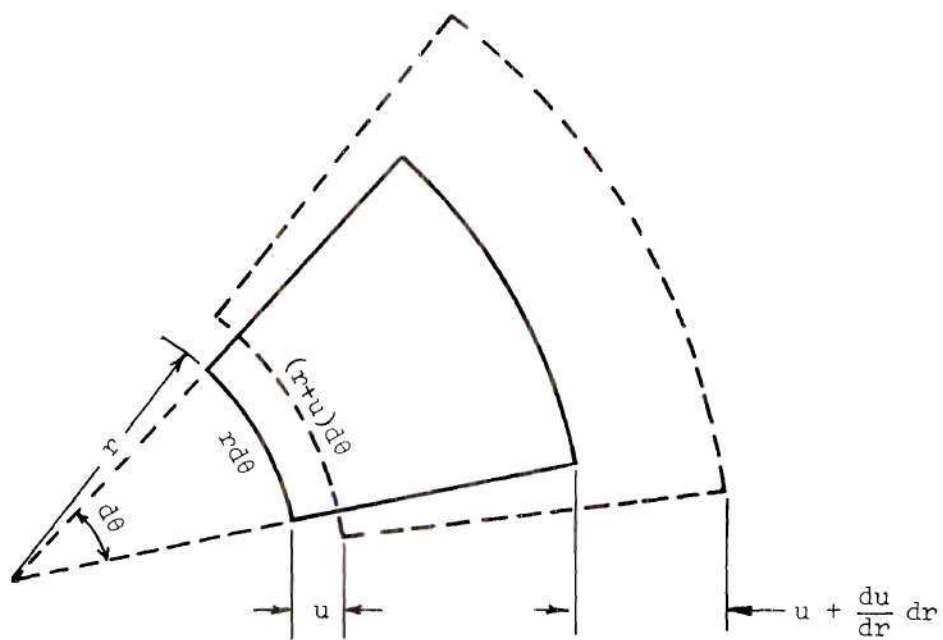


Figure 5. Deformation in Polar Coordinates

$$\epsilon_{\theta} = \frac{\Delta L_{\theta}}{L_{\theta}} = \frac{(r+u)d\theta - rd\theta}{rd\theta} = \frac{u}{r}$$

Both ϵ_{θ} and ϵ_r are functions of a single variable, r . They are not independent and must be related to one another in some fashion. If ϵ_{θ} is differentiated with respect to r

$$\frac{d\epsilon_{\theta}}{dr} = \frac{du}{dr} \frac{1}{r} - \frac{u}{r^2}$$

Rewritten as

$$r \frac{d\epsilon_{\theta}}{dr} = \epsilon_r - \epsilon_{\theta}$$

This is the compatibility relation for a cylinder. Note that the preceding equations are independent of end conditions or boundary conditions. The only requirement is that the deformations are symmetrical about the axis. For the solution it is necessary to introduce a stress-strain relationship. In the elastic region Hooke's Law is that relationship. In the plastic region it is necessary to use the Prandtl-Reuss or the Levy-Mises stress-strain relations.

Elastic Solution for a Cylinder With Internal Pressure P

Hooke's Law is

$$\epsilon_r = \frac{1}{E} [\sigma_r - \nu(\sigma_{\theta} + \sigma_z)] \quad (1)$$

$$\epsilon_{\theta} = \frac{1}{E} [\sigma_{\theta} - \nu(\sigma_r + \sigma_z)]$$

$$\epsilon_z = \frac{1}{E} [\sigma_z - \nu(\sigma_r + \sigma_{\theta})]$$

Written in terms of stresses,

$$\sigma_r = \frac{E}{1 - \nu^2} (\epsilon_r + \nu\epsilon_{\theta}) + \frac{\nu}{1 - \nu} \sigma_z \quad (2)$$

$$\sigma_{\theta} = \frac{E}{1 - \nu^2} (\nu\epsilon_r + \epsilon_{\theta}) + \frac{\nu}{1 - \nu} \sigma_z$$

From the strain-displacement relationships

$$\epsilon_r = \frac{du}{dr}$$

$$\epsilon_{\theta} = \frac{u}{r}$$

Then:

$$\sigma_r = \frac{E}{1 - \nu^2} \left(\frac{du}{dr} + \nu \frac{u}{r} \right) + \frac{\nu}{1 - \nu} \sigma_z \quad (3)$$

$$\sigma_{\theta} = \frac{E}{1 - \nu^2} \left(\nu \frac{du}{dr} + \frac{u}{r} \right) + \frac{\nu}{1 - \nu} \sigma_z$$

Substitute these values into the equilibrium equation.

$$\frac{d^2 u}{dr^2} + \frac{1}{r} \frac{du}{dr} - \frac{u}{r^2} = 0 \quad (4)$$

for which $u = Ar + \frac{B}{r}$ is a solution.

$$\epsilon_r = \frac{du}{dr} = A - \frac{B}{r^2}$$

$$\epsilon_\theta = \frac{u}{r} = A + \frac{B}{r^2}$$

Substitute into Hooke's Law (1).

$$E \left(A + \frac{B}{r^2} \right) = \sigma_r - \nu \sigma_\theta$$

$$E \left(A + \frac{B}{r^2} \right) = \sigma_\theta - \nu \sigma_r - \nu \sigma_z$$

$$E(\epsilon_z) = \sigma_z - \nu \sigma_r - \nu \sigma_\theta$$

Solve these equations simultaneously for σ_r , σ_θ , and σ_z .

$$(1+\nu)(1-2\nu) \frac{\sigma_r}{E} = A - (1-2\nu) \frac{B}{r^2} + \nu \epsilon_z \quad (5)$$

$$(1+\nu)(1-2\nu) \frac{\sigma_\theta}{E} = A + (1-2\nu) \frac{B}{r^2} + \nu \epsilon_z$$

$$(1+\nu)(1-2\nu) \frac{\sigma_z}{E} = 2\nu A + (1-\nu) \epsilon_z$$

To evaluate A and B the boundary conditions are:

$$\text{when } r = b \quad \sigma_r = 0 \quad (\text{free surface})$$

$$\text{when } r = a \quad \sigma_r = -P$$

Solve for A and B using these boundary conditions and substitute into Equations (2)

$$\sigma_r = \frac{a^2 P}{b^2 - a^2} \left(1 - \frac{b^2}{r^2} \right) \quad (6)$$

$$\sigma_\theta = \frac{a^2 P}{b^2 - a^2} \left(1 + \frac{b^2}{r^2} \right)$$

$$\sigma_z = E\epsilon_z + \frac{2\nu Pa^2}{b^2 - a^2}$$

For a closed end cylinder

$$\sigma_z = \frac{Pa^2}{b^2 - a^2}$$

For an open end cylinder

$$\sigma_z = 0$$

For a fixed end cylinder $\epsilon_z = 0$ and

$$\sigma_z = \frac{2\nu Pa^2}{b^2 - a^2}$$

Yield Conditions

In order to determine the stresses in an elastic-plastic cylinder it is necessary to determine at what stress level yielding occurs. With combined stresses it is not sufficient to say yielding is initiated when any one of the principal stresses reaches the yield point, but rather when some combination of the principal stresses reaches the yield point. The theories of yielding commonly used are the maximum shear stress or Tresca theory and the von Mises or distortion energy theory.

The Maximum Shear Stress, proposed by Tresca and Saint-Venant, states that plastic yielding occurs when

$$\tau_{\max} = \frac{\sigma_1 - \sigma_3}{2}$$

reaches a critical value. Both in uniaxial tension and uniaxial compression the maximum shearing stress is $\sigma_o/2$. σ_o is the yield point of the material in simple tension or compression. Hence the yield condition can be stated as

$$\tau_{\max} = \frac{\sigma_1 - \sigma_3}{2} = \frac{\sigma_o}{2}$$

or

$$\sigma_1 - \sigma_3 = \sigma_o$$

where σ_1 is the largest principal stress and σ_3 is the smallest.

The distortion energy condition introduced by von Mises states yielding occurs when the quantity

$$U' = \frac{1}{12G} [(\sigma_1 - \sigma_2)^2 + (\sigma_1 - \sigma_3)^2 + (\sigma_2 - \sigma_3)^2]$$

reaches a critical value.

For uniaxial loading the distortion energy becomes

$$U' = \frac{\sigma_o^2}{6G}$$

and the yield condition is then

$$\sigma_o = \frac{1}{\sqrt{2}} \sqrt{(\sigma_1 - \sigma_2)^2 + (\sigma_1 - \sigma_3)^2 + (\sigma_2 - \sigma_3)^2}$$

Plastic Deformation of a Cylinder

Hoffman-Sachs Solution

For the case of plane strain the so-called critical pressure, at which plastic flow commences, can be determined using the distortion energy criterion for yielding. The distortion energy condition for a cylinder is

$$(\sigma_r - \sigma_\theta)^2 + (\sigma_\theta - \sigma_z)^2 + (\sigma_r - \sigma_z)^2 = 2\sigma_o^2$$

which by substituting values from Equations (6) becomes

$$P \frac{2a^2/r^2}{1 - a^2/b^2} = \frac{2}{3} \sigma_o$$

The expression on the left will be greatest at the inner surface $r = a$ thus giving the critical pressure P_c at which yielding of the cylinder is initiated.

$$P_c = \frac{1 - a^2/b^2}{3} \sigma_o$$

To investigate the progress of the plastic front from the inner face to the outer face of the tube when the pressure is greater than the critical pressure consider a value ρ , the radius of the elastic-plastic interface. Conditions throughout the plastic region are governed by the von Mises condition for yielding and by the Levy-Mises theory of plastic flow,

$$\frac{d\epsilon_z}{d\epsilon_r} = \frac{2\sigma_z - \sigma_r - \sigma_\theta}{2\sigma_r - \sigma_\theta - \sigma_z}$$

Recall that for plane strain $\epsilon_z = 0$ and consequently $d\epsilon_z = 0$ gives

$$2\sigma_z - \sigma_r - \sigma_\theta = 0$$

manipulating

$$\sigma_z = \frac{\sigma_r + \sigma_\theta}{2}$$

Substitute this value of σ_z into the von Mises yield criterion and get

$$\sigma_\theta - \sigma_r = \frac{2}{\sqrt{3}} \sigma_o \quad (7)$$

The differential equation of equilibrium becomes

$$\frac{d\sigma_r}{dr} - \frac{2}{\sqrt{3}} \frac{\sigma_o}{r} = 0$$

A solution to this equation is

$$\sigma_r = \frac{2\sigma_o}{\sqrt{3}} \ln r + C \quad (8)$$

The constant of integration C is determined from the condition that the stress σ_r is continuous across the elastic-plastic interface at radius ρ . The stress in the plastic region is

$$(\sigma_r)_{r=\rho} = \frac{2\sigma_o}{\sqrt{3}} \ln \rho + C$$

At the elastic-plastic interface the material is in a state of incipient yielding. Thus

$$P_c = \frac{\sigma_o}{3} \left(1 - \frac{\rho^2}{b^2} \right)$$

and since at ρ $\sigma_r = P_c$ the two values of σ_r can be equated.

$$\frac{2\sigma_o}{3} \ln \rho + c = \frac{\sigma_o}{\sqrt{3}} \left(1 - \frac{\rho^2}{b^2} \right)$$

From this equation

$$c = - \frac{\sigma_o}{\sqrt{3}} \left(2 \ln \rho + 1 - \frac{\rho^2}{b^2} \right)$$

and entering with this value of C into Equation (8) one has

$$\sigma_r = \frac{\sigma_o}{\sqrt{3}} \left(2 \ln \frac{r}{\rho} - 1 + \frac{\rho^2}{b^2} \right) \quad (9)$$

and from Equation (7)

$$\sigma_\theta = \frac{\sigma_o}{\sqrt{3}} \left(2 \ln \frac{r}{\rho} + 1 + \frac{\rho^2}{b^2} \right)$$

$$\sigma_z = \frac{\sigma_o}{\sqrt{3}} \left(2 \ln \frac{r}{\rho} + \frac{\rho^2}{b^2} \right)$$

The above equations furnish stresses in the plastic region. For the outer elastic shell the stresses are obtained by substituting for P the critical pressure needed to cause yielding at ρ .

$$P_c = \frac{\sigma_o}{\sqrt{3}} \left(1 - \frac{\rho^2}{b^2} \right)$$

Then

$$\sigma_r = \frac{\sigma_o}{\sqrt{3}} \left(\frac{\rho^2}{b^2} - \frac{\rho^2}{r^2} \right) \quad (10)$$

$$\sigma_\theta = \frac{\sigma_o}{\sqrt{3}} \left(\frac{\rho^2}{b^2} + \frac{\rho^2}{r^2} \right)$$

$$\sigma_z = \frac{\sigma_o}{\sqrt{3}} \left(\frac{\rho^2}{b^2} \right)$$

To find the relationship between the applied pressure p and the radius of the elastic-plastic interface ρ , recall that at $r = a$ the stress $\sigma_r = -P$ and

$$P = \frac{\sigma_o}{\sqrt{3}} \left(2 \ln \frac{\rho}{a} + 1 - \frac{\rho^2}{b^2} \right)$$

For any value of P , ρ can be found by an iterative procedure.

Coffin-MacGregor Partially Plastic Solution (4)

Coffin-MacGregor et al. have developed a numerical method of calculating the autofrettage stresses in an open end cylinder. The basic assumptions for the material within the cylinder are:

1. *Law of Yielding* $(\sigma_r - \sigma_t)^2 + (\sigma_r - \sigma_z)^2 + (\sigma_z - \sigma_t)^2 = 2\sigma_o^2$
2. *Equilibrium* $r = r \frac{d\sigma_r}{dr} = \sigma_t - \sigma_r$

3. *Compatibility of Strains* $r \frac{d\epsilon_t}{dr} = \epsilon_r - \epsilon_t$

4. *Elastic Compressibility* $\epsilon_r + \epsilon_t + \epsilon_z = \frac{1 - 2\nu}{E} (\sigma_r + \sigma_t + \sigma_z)$

5. *Constant Axial Strain* $\epsilon_z = k$

6. All stresses and strains are continuous across the elastic-plastic interface.

7. Total end load of the cylinder must be zero.

$$Z = 2\pi \int_{r_i}^{r_o} \sigma_z r dr = 0$$

8. The material obeys a perfectly plastic stress-strain relationship.

9. There is an elastic region where the stress-strain relationship is given by the ordinary elastic equations.

From the above-mentioned assumptions, the following differential equations for the stress and a quantity D may be derived.

$$\sigma'_r = \sigma_t - \sigma_r$$

$$\sigma'_t = \frac{(W_z - W_l)a_z^2 - W_l a_r a_t}{(\text{DENOM})} (\sigma_t - \sigma_r).$$

$$\sigma'_z = \frac{(a_t - a_r)(a_z W_l + z_t W_2)}{(\text{DENOM})} (\sigma_t - \sigma_r)$$

$$D = \frac{(W_2^2 - W_l^2)(a_t - a_r)}{(\text{DENOM})} (\sigma_t - \sigma_r)$$

where $\sigma_r, \sigma_t, \sigma_z$ = the stresses in the radial, tangential and axial directions.

$\epsilon_r, \epsilon_t, \epsilon_z$ = the strains in the radial, tangential and axial directions.

$\sigma'_r, \sigma'_t, \sigma'_z$ = derivatives of the principal stresses with respect to the radius r .

$$(\text{DENOM}) = (a_t^2 + a_z^2)W_1 + 2a_t a_z W_2$$

$$W_1 = 1 + D$$

$$W_2 = \nu + D/2$$

$$a_r = \sigma_r - \frac{1}{2} (\sigma_t + \sigma_z)$$

$$a_t = \sigma_t - \frac{1}{2} (\sigma_r + \sigma_z)$$

$$a_z = \sigma_z - \frac{1}{2} (\sigma_r + \sigma_t)$$

These differential equations can be solved numerically to give values of σ_r , σ_t , σ_z and D for any ratio of radii and any depth of yielding. The values σ_r/σ_o , σ_t/σ_o , σ_z/σ_o and D where σ_o is the yield strength are given in tables for $1 \leq r_o/r_i \leq 4$ and $1 \leq r_o/r \leq r_o/r_i$ in reference (4).

The strains may be computed from the relationships

$$E\epsilon_r = (1+D)\sigma_r - (\nu+D/2)(\sigma_t + \sigma_z)$$

$$E\epsilon_t = (1+D)\sigma_t - (v+D/2)(\sigma_r + \sigma_z)$$

$$E\epsilon_z = (1+D)\sigma_z - (v+D/2)(\sigma_r + \sigma_t)$$

The stresses in the elastic region are

$$\sigma_r = \frac{1}{2} (\sigma_{rp} + \sigma_{tp}) \left[1 - \left(\frac{r_o}{r} \right)^2 \right]$$

$$\sigma_t = \frac{1}{2} (\sigma_{rp} + \sigma_{tp}) \left[1 + \left(\frac{r_o}{r} \right)^2 \right]$$

$$\sigma_z = \sigma_{zp}$$

where the p subscript denotes the value of the stresses at $r = r_p$, the elastic-plastic interface.

Thermal Stress Analysis

Mendelson and Manson Procedure (5,6)

The Mendelson and Manson procedure modified by Johnson is essentially a numerical iterative solution involving simultaneous solution of the equilibrium, compatibility and stress-strain equations. Mendelson and Manson have developed the method of successive approximations for a solid circular cylinder in terms of integral equations. Johnson has modified the Mendelson and Manson technique to solve for the stress state in a hollow cylinder and has written the equations in finite difference form.

The analysis of a long hollow circular cylinder is subject to the following assumptions:

1. The cylinder material is linearly elastic up to the elastic limit; beyond this point, plastic flow occurs.
2. Axial symmetry exists.
3. ϵ_z is a constant.
4. Steady state conditions are present as far as heat flow is concerned.
5. Calculations are made at a sufficient distance from the ends so that end conditions are negligible.
6. The cylinder is subjected to internal pressure and is without axial restraint.
7. The coefficient of thermal expansion and the modulus of elasticity vary in a known manner with temperature.
8. Poisson's ratio is a constant.
9. The deformation theory of plasticity with the von Mises yield condition is used.

The determination of stresses and strains in a long cylinder follows the usual treatment for plane strain problems; the equilibrium equation is given by

$$\frac{d\sigma_r}{dr} + \frac{\sigma_r - \sigma_\theta}{r} = 0 \quad (11)$$

The compatibility equation is

$$\frac{d\epsilon_\theta}{dr} + \frac{\epsilon_\theta - \epsilon_r}{r} = 0 \quad (12)$$

and the stress strain equations are

$$\begin{aligned}\epsilon_r &= \frac{1}{E} [\sigma_r - \nu(\sigma_\theta + \sigma_z)] + \alpha T + \epsilon_{rp} \\ \epsilon_\theta &= \frac{1}{E} [\sigma_\theta - \nu(\sigma_r + \sigma_z)] + \alpha T + \epsilon_{\theta p} \\ \epsilon_z &= \frac{1}{E} [\sigma_z - \nu(\sigma_r + \sigma_\theta)] + \alpha T + \epsilon_{zp}\end{aligned}\tag{13}$$

Writing Equation (12) in terms of stresses by use of Equation (13) gives

$$\begin{aligned}\frac{d}{dr} \left[\frac{1}{E} \sigma_\theta - \frac{\nu}{E} \sigma_r - \frac{\nu}{E} \sigma_z + \alpha T + \epsilon_{\theta p} \right] &= \frac{1+\nu}{E_r} (\sigma_r - \sigma_\theta) \\ &+ \frac{\epsilon_{rp} - \epsilon_{\theta p}}{r}\end{aligned}\tag{14}$$

Also solving the last of Equation (13) for ϵ_z and substituting in Equation (14) gives

$$\begin{aligned}\frac{d}{dr} \left[\frac{1}{E} \sigma_\theta - \frac{\nu}{E} \sigma_r - M\epsilon_z - \frac{\nu^2}{E} (\sigma_r + \sigma_\theta) + \nu\alpha T + \nu\epsilon_{zp} \right. \\ \left. + \alpha T + \epsilon_{\theta p} \right] &= \frac{1+\nu}{E_r} (\sigma_r - \sigma_\theta) + \frac{\epsilon_{rp} - \epsilon_{\theta p}}{r}\end{aligned}\tag{15}$$

For the generalized plane strain problem ϵ_z is a constant and is determined from the axial loading on the cylinder as follows:

$$\int_a^b \sigma_z r dr = \frac{a_P^2}{2}$$

or

$$\int_a^b [E\epsilon_z + v(\sigma_r + \sigma_\theta) - E\alpha T - E\epsilon_{zP}] r dr = \frac{a_P^2}{2}$$

Therefore

$$\epsilon_z = \frac{\frac{a_P^2}{2} - \int_a^b [v(\sigma_r + \sigma_\theta) - E\alpha T - E\epsilon_{zP}] r dr}{\int_a^b E r dr} \quad (17)$$

Substituting Equation (17) into Equation (15) gives a pair of simultaneous differential Equations (11) and (15) which can be solved for σ_r and σ_θ .

In the finite difference method a number of discrete point stations are chosen along the radius. It is assumed that at each of the points the plastic strains, the temperature, the quantities ϵ , α , and v are known, and also that the values of these quantities can be approximated midway between these point stations. Using middle differences, let

$$\left. \frac{d\sigma}{dr} \right|_{n-\frac{1}{2}} = \frac{\sigma_n - \sigma_{n-1}}{r_n - r_{n-1}} \quad \text{and} \quad \sigma \Big|_{n+\frac{1}{2}} = \frac{\sigma_n + \sigma_{n+1}}{2}$$

Substituting this and similar relations for other quantities into

Equations (11) and (15),

$$C_n \sigma_{rn} - D_n \sigma_{\theta n} = F_n \sigma_{rn-1} + G_n \sigma_{\theta n-1}$$

and

$$C'_n \sigma_{rn} + D'_n \sigma_{\theta n} = F'_n \sigma_{rn-1} + G'_n \sigma_{\theta n-1} + H'_n + P'_n \quad (19)$$

where

$$C_n = \frac{1}{h_n} + \frac{1}{2r_n}$$

$$C'_n = -\frac{v}{(hE)_n} - \frac{v^2}{(hE)_n} - \frac{1+v}{2E_n r_n}$$

$$D_n = \frac{1}{2r_n}$$

$$D'_n = \frac{1}{(hE)_n} - \frac{v^2}{(hE)_n} + \frac{1+v}{2E_n r_n}$$

$$F_n = \frac{1}{h} - \frac{1}{2r_{n-1}}$$

$$F'_n = \frac{v}{(hE)_{n-1}} - \frac{v^2}{(hE)_{n-1}} + \frac{1+v}{2E_{n-1} r_{n-1}}$$

$$G_n = \frac{1}{2r_{n-1}}$$

$$G'_n = \frac{1}{(hE)_{n-1}} - \frac{v^2}{(hE)_{n-1}} - \frac{1+v}{2E_{n-1} r_{n-1}}$$

$$H'_n = \frac{1+v}{h_n} [(\alpha T)_n - (\alpha T)_{n-1}]$$

$$P'_n = \left(-\frac{1}{h_n} - \frac{1}{2r_n} + \frac{v}{h_n} \right) \epsilon_{\theta pn} + \left(\frac{1}{2r_n} + \frac{v}{h_n} \right) \epsilon_{rpn} + \left(\frac{1}{h_n} - \frac{1}{2r_{n-1}} - \frac{v}{h_n} \right) \epsilon_{pn-1} \\ + \left(\frac{1}{2r_{n-1}} - \frac{v}{h_n} \right) \epsilon_{rpn-1}$$

Considering the linear nature of Equations (18) and (19) and the possibility of successive application of these equations in going from station to station, it follows that the stresses at any station can ultimately be expressed in linear terms of the stresses at any other station. For convenience, the stresses at all stations are expressed in terms of the tangential stress at the inner radius $\sigma_{\theta a}$; thus,

$$\sigma_{rn} = A_{rn} \sigma_{\theta a} + B_{rn} \quad (20)$$

$$\sigma_{\theta n} = A_{\theta n} \sigma_{\theta a} + B_{\theta n} \quad (21)$$

$$\sigma_{rn-1} = A_{rn-1} \sigma_{\theta a} + B_{rn-1} \quad (22)$$

$$\sigma_{\theta n-1} = A_{\theta n-1} \sigma_{\theta a} + B_{\theta n-1} \quad (23)$$

Substituting these values of σ_{rn} , $\sigma_{\theta n}$, σ_{rn-1} , and $\sigma_{\theta n-1}$ into Equations (18) and (19),

$$\begin{aligned} & (C_n A_{rn} - D_n A_{\theta n} - F_n A_{rn-1} - G_n A_{\theta n-1}) \sigma_{\theta a} + (C_n B_{rn} \\ & - D_n B_{\theta n} - F_n B_{rn-1} - G_n B_{\theta n-1}) = 0 \end{aligned} \quad (24)$$

$$(C'_n B_{rn} - D'_n B_{\theta n} - F'_n B_{rn-1} - G'_n B_{\theta n-1} - H'_n - P'_n) = 0 \quad (25)$$

In Equations (24) and (25) the stress $\sigma_{\theta}(a)$ is completely arbitrary, since it depends only upon the boundary conditions and not on

the equations of elasticity. Thus, the equations are valid for any value of $\sigma_\theta(a)$. For this to be true, the terms in the parentheses must equal zero. Therefore,

$$\begin{aligned} C_n A_{rn} - D_n A_{\theta n} - F_n A_{rn-1} - G_n A_{\theta n-1} &= 0 \\ C_n B_{rn} - D_n B_{\theta n} - F_n B_{rn-1} - G_n B_{\theta n-1} &= 0 \end{aligned} \quad (26)$$

$$C'_n A_{rn} - D'_n A_{\theta n} - F'_n A_{rn-1} - G'_n A_{\theta n-1} = 0$$

$$C'_n B_{rn} - D'_n B_{\theta n} - F'_n B_{rn-1} - G'_n B_{\theta n-1} + H'_n + P'_n = 0$$

Solving these four equations simultaneously for A_{rn} , $A_{\theta n}$, B_{rn} , and $B_{\theta n}$,

$$A_{rn} = K A_{rn-1} + L A_{\theta n-1}$$

$$A_{\theta n} = K' A_{rn-1} + L' A_{\theta n-1}$$

(27)

$$B_{rn} = K B_{rn-1} + L B_{\theta n-1} + M_n$$

$$B_{\theta n} = K' B_{rn-1} + L' B_{\theta n-1} + M'_n$$

where

$$K_n = \frac{D'_n F_n + D_n F'_n}{C_n D'_n + D'_n D_n}$$

$$K'_n = \frac{C_n F'_n - C'_n F_n}{C_n D'_n + D'_n D_n}$$

$$L_n = \frac{D'_n G_n + D_n G'_n}{C_n D'_n + C'_n D_n}$$

$$L'_n = \frac{C_n G'_n - C'_n G_n}{C_n D'_n + C'_n D_n}$$

$$M_n = \frac{D_n (H'_n + P'_n)}{C_n D'_n + C'_n D_n}$$

$$M'_n = \frac{C_n (H'_n + P'_n)}{C_n D'_n + C'_n D_n}$$

At $r = a$ (station 1, inside surface), $\sigma_{ra} = 0$ (boundary condition) and $\sigma_{\theta n} = \sigma_{\theta a}$. Substituting in Equations (20) and (21),

$$0 = A_{ra} \sigma_{\theta a} + B_{ra}$$

$$\sigma_{\theta a} = A_{\theta a} \sigma_{\theta a} + B_{\theta a}$$

These equations are true regardless of the value of $\sigma_{\theta a}$. Therefore,

$$B_{\theta a} = 0$$

$$A_{\theta a} = 1$$

(28)

$$A_{ra} = 0$$

$$B_{ra} = 0$$

The radial stress at the outside surface ≈ 0 (boundary condition).
Therefore,

$$\sigma_{rb} = 0 = A_{rb} \sigma_{\theta a} + B_{rb}$$

or

$$\sigma_{\theta a} = \frac{B_{rb}}{A_{rb}} \quad (29)$$

From the known coefficients at the first station (Equation (28)), the coefficients at all other stations can be determined progressively by successive applications of Equation (27). When all of the coefficients have been determined, the unknown σ_{θ} can be determined from Equation (29). Then the radial and tangential stresses can be determined at each station using Equations (20) and (21).

The plastic strains are given by the equations

$$\begin{aligned} \epsilon_{rp} &= \frac{\epsilon_{ep}}{3\epsilon_{et}} (2\epsilon_r - \epsilon_{\theta} - \epsilon_z) \\ \epsilon_{\theta p} &= \frac{\epsilon_{ep}}{3\epsilon_{et}} (2\epsilon_{\theta} - \epsilon_r - \epsilon_z) \end{aligned} \quad (30)$$

$$\epsilon_{zp} = -\epsilon_{rp} - \epsilon_{\theta p}$$

where

$$\epsilon_{et} = \frac{\sqrt{2}}{3} \sqrt{(\epsilon_r - \epsilon_{\theta})^2 + (\epsilon_r - \epsilon_z)^2 + (\epsilon_{\theta} - \epsilon_z)^2} \quad (31)$$

and the equivalent plastic strain ϵ_{ep} is related through the stress-strain curve of the material by the following relation:

$$\epsilon_{et} = \frac{2}{3} \frac{\sigma_e}{E} (1+\nu) + \epsilon_{ep} \quad (32)$$

where σ_e is the equivalent stress and is

$$\sigma_e = \frac{1}{\sqrt{2}} \sqrt{(\sigma_r - \sigma_\theta)^2 + (\sigma_r - \sigma_z)^2 + (\sigma_\theta - \sigma_z)^2} \quad (33)$$

The Method of Calculation can be summarized as follows:

1. Assume values of the plastic strains usually zero everywhere.
2. Solve Equations (11) and (15) by the finite difference method.
3. Calculate the total strains by means of Equations (13).
4. Calculate ϵ_z from Equation (17) using an appropriate technique such as Simpson's Rule of Numerical Integration.
5. Calculate the equivalent total strain ϵ_{et} from Equation (31).
6. Calculate ϵ_{ep} from Equation (32).
7. Calculate ϵ_{rp} , $\epsilon_{\theta p}$ and ϵ_{zp} from Equations (30).
8. Using these values of plastic strain, go back to step 2.
9. Continue until convergence is obtained.

Experimental Determination

There are several ways of determining the residual or rest stresses in a system. These stresses may result from non-uniform distribution of plastic strain such as is found in autofrettaged guns.

Nearly all methods of residual stress determination are destructive in nature. A non-destructive stress determination may be accomplished on the surface of the specimen by means of X-rays, but if a

stress distribution throughout a test piece is required, it is necessary to machine away part of the surface, to create new surfaces on which the X-rays may act. Most methods of stress determination are approximate in nature. While there are several methods available for determination of uniaxial or biaxial states of stress, there appears to be only one generally accepted method for determination of a triaxial state of stress, and this may be applied only to rods, cylinders and thick-walled tubes. This process is the Sachs' boring out method.

Sachs' Boring Out Method

This method developed by Sachs (7) takes account of all three principal stresses and assumes only that they have rotational symmetry and are uniform along the length of the specimen. The method consists of measuring the change of length and diameter of the tube as the inside is bored out in steps; a measurement being made after each boring operation. The tube should have a length some three times its diameter. The length and diameter measurements should be taken at several places around the object and averaged.

The residual stresses locked in the body may be determined by the following equations.

$$\sigma_z = \frac{E}{1 - \nu^2} \left[(F_b - F) \frac{d\lambda}{dF} - \lambda \right] \quad (34)$$

$$\sigma_t = \frac{E}{1 - \nu^2} \left[(F_b - F) \frac{d\theta}{dF} - \frac{(F_b + F)}{2F} \theta \right] \quad (35)$$

$$\sigma_r = \frac{E}{1 - \nu^2} \left[\frac{(F_b - F)}{2F} \theta \right] \quad (36)$$

where $\sigma_r, \sigma_t, \sigma_z$ = the radial, tangential and axial stresses corresponding to the area F .

ν = Poisson's Ratio taken as 0.3 for gun steel.

E = modulus of elasticity taken as 30×10^6 psi for gun steel.

ϵ_z = axial strain.

ϵ_t = tangential strain.

$\theta = \epsilon_t + \nu \epsilon_z$.

$\Lambda = \epsilon_z + \nu \epsilon_t$.

F_b = cross sectional area of the original cylinder = $\pi D_o^2/4$.

F = area calculated from the inside diameter D_i after boring each layer = $\pi D_i^2/4$.

The experimentally determined data may be smoothed by plotting the quantities ϵ_z , ϵ_t , Λ and θ against the area F and then by drawing smooth curves through as many of the data points as is practical. The slopes required in the calculation procedure $d\Lambda/df$ and $\frac{d\theta}{dF}$ may be taken from these smooth curves.

It is essential that machining operations be done with great care. The cutting tool should be sharp to minimize cold working and heating effects. Measurements of strain should be made at constant temperature, or adequate corrections should be made for temperature changes found at the time of strain measurement.

When the entire operation is finished, there are general tests which may be applied to the results in order to give an indication of their reliability.

1. On a plot of longitudinal stress σ_z against the cross section of the bore the areas under the curves that represent compression should

be equal to those that represent tension.

2. Equal compressive and tensile areas should be found on the tangential stress σ_t plot.

3. The residual radial stress σ_r should of necessity be zero at the inner and outer surfaces.

CHAPTER III

ANALYTICAL RESULTS

The Mendelson and Manson method of successive approximations is not the only solution considered in this study. The solution of D. R. Bland, which is a closed form solution, was considered and rejected because in the Bland solution the axial stress is assumed to be in magnitude between the radial and tangential stresses. This assumption is indeed valid for a wide range of conditions. This assumption allows use of the Tresca or Maximum Shear Stress yield criterion which facilitates solving the equilibrium equation.

An elastic thermal stress analysis, the results of which are given in Table 3, clearly show that the axial stress is somewhat larger than the tangential stress. Thus, it is necessary to utilize the von Mises yield criterion which considers all three principal stresses. The Mendelson and Manson method incorporates the von Mises yield criterion and was subsequently chosen to calculate the states of stress and strain, both autofrettage and thermal.

Variable Properties

In any solution to a thermal stress problem, it is desirable to include provisions for the temperature dependency of the physical properties of the material, Young's modulus, coefficient of thermal expansion and yield strength. The particular steel of which the gun was manufactured is a ferritic steel of the following composition:

0.04% C, 0.64% Mn, 0.26% Si, 0.028% P, 0.037% S, 0.10% Cr, 0.22% Ni, 0.55% Mo, and 0.11% V and has yield strength of 75,000 psi.

The difficulties in finding data giving temperature dependence of the properties of any particular steel were compounded in this case by the fact that the steel was a war time melt. The forging of the gun barrel was completed in 1943. No records are available giving the variation of the physical constants with temperature, if tests were carried out to evaluate temperature dependency. Attempts were made to approximate the values for the coefficient of thermal expansion with data generated from tests of a steel of similar composition (9). Rather than guess at a yield strength-temperature relationship, a constant yield strength of 75,000 psi was used for all temperatures.

In the paper by Roberts and Nortcliffe (10), a description was given of vibrational method for determination of Young's modulus which is particularly convenient for measurements at high temperatures. Results at temperatures up to 1000°C were given for several ferritic steels. It was subsequently noticed that the variations of Young's modulus with temperature, up to 600°C, were practically identical, regardless of the composition of the steel. Hoyt gives slightly different values for the effects of temperature on the elastic moduli of steels (11).

Solutions were generated using both the data from Nortcliffe and Jones and the data from Hoyt. While the differences were small, solutions using the data of Hoyt appeared to give better correlation with the experimental results.

Residual Autofrettage Stresses

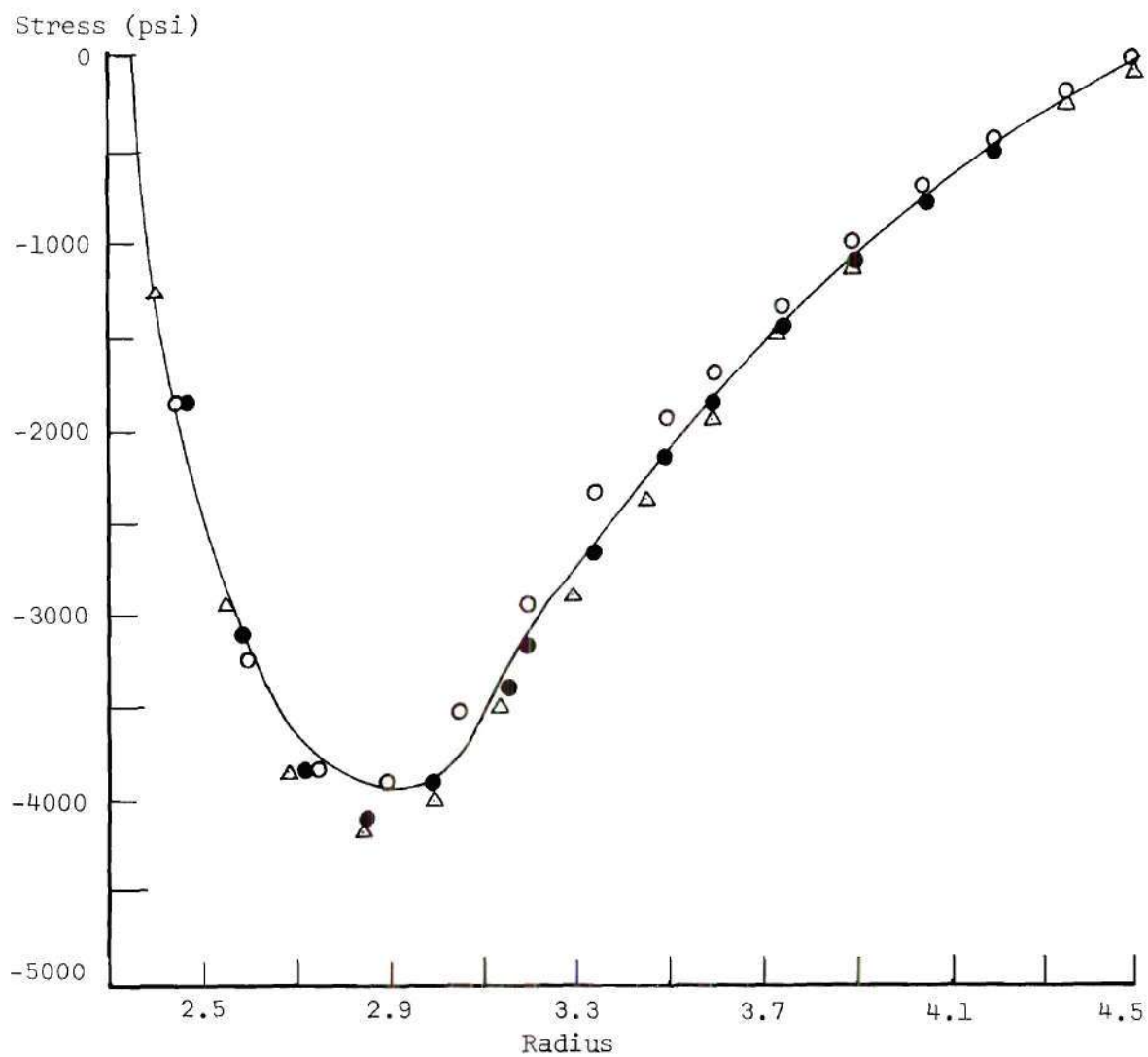
Residual stresses arise from the fact that not all of the material is permanently deformed the same amount. In an elastic-plastic cylinder, such as an autofrettaged gun barrel, the elastic portion is, of course, not permanently deformed at all. When the load is removed, it is assumed that the cylinder unloads elastically. The cylinder will not return to its original dimensions due to the plastic deformation, thus inducing a state of residual stress.

The rest or residual stresses introduced by the autofrettage process may be obtained by subtracting from the elastic-plastic action stresses equivalent purely elastic stresses due to the same internal pressure, P . The elastic-plastic action stresses are calculated by the Sachs closed form solution or by the Coffin-MacGregor numerical solution.

The elastic stresses to be subtracted are arrived at by the Timoshenko solution for a thick-walled cylinder as given in section 1 of Chapter II.

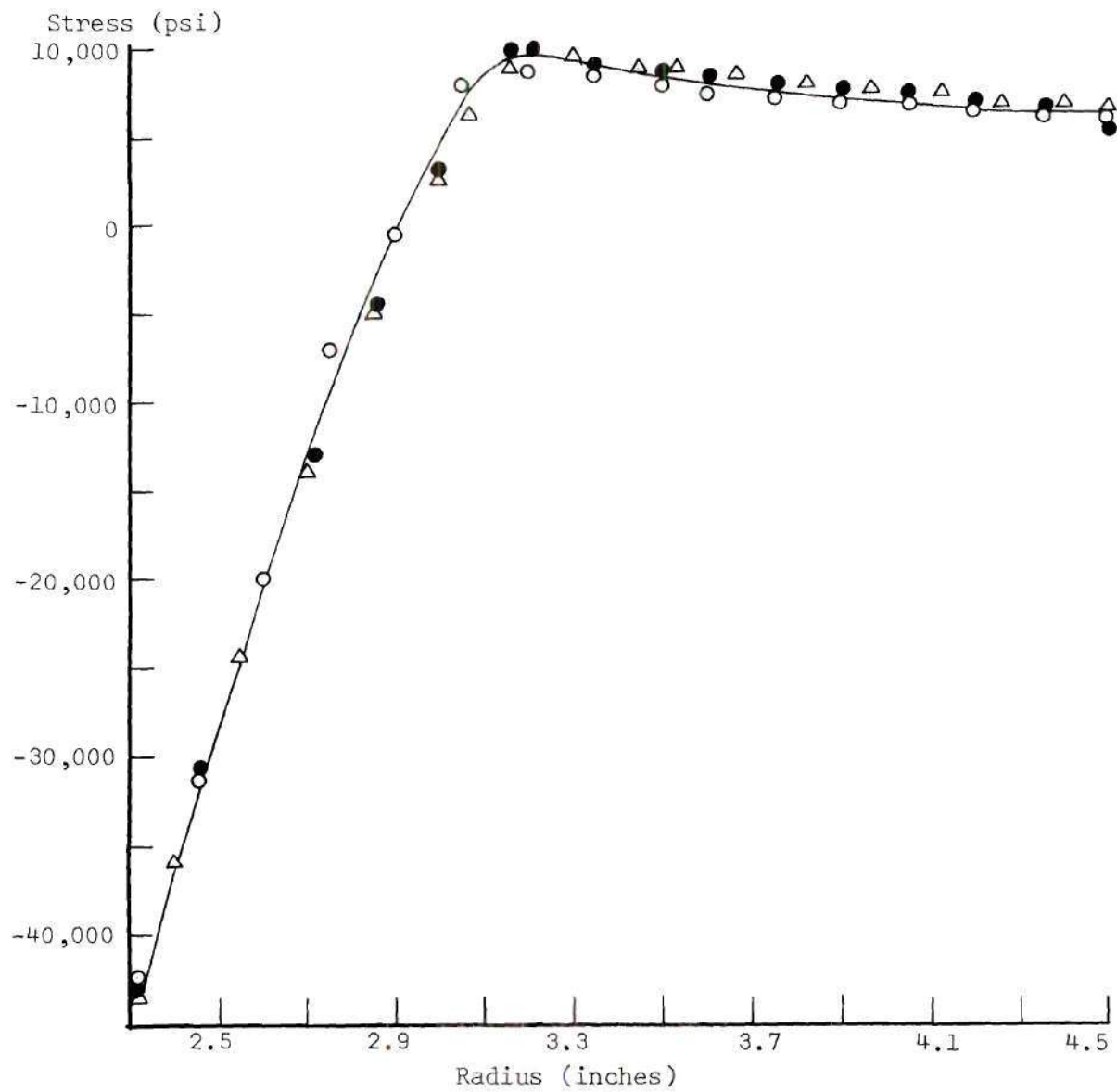
The residual autofrettage stresses calculated in this fashion from the Sachs and Coffin-MacGregor action stress solution are given in Figures 6, 7, and 8. Also in Figures 6, 7, and 8 are the residual autofrettage stresses calculated from the Mendelson and Manson method.

The Mendelson and Manson solution, for which a computer is required, calculated the residual stresses by first calculating the permanent deformation caused by the pressure P , then reducing the load to zero. The advantage of this method is if there is any reyielding of



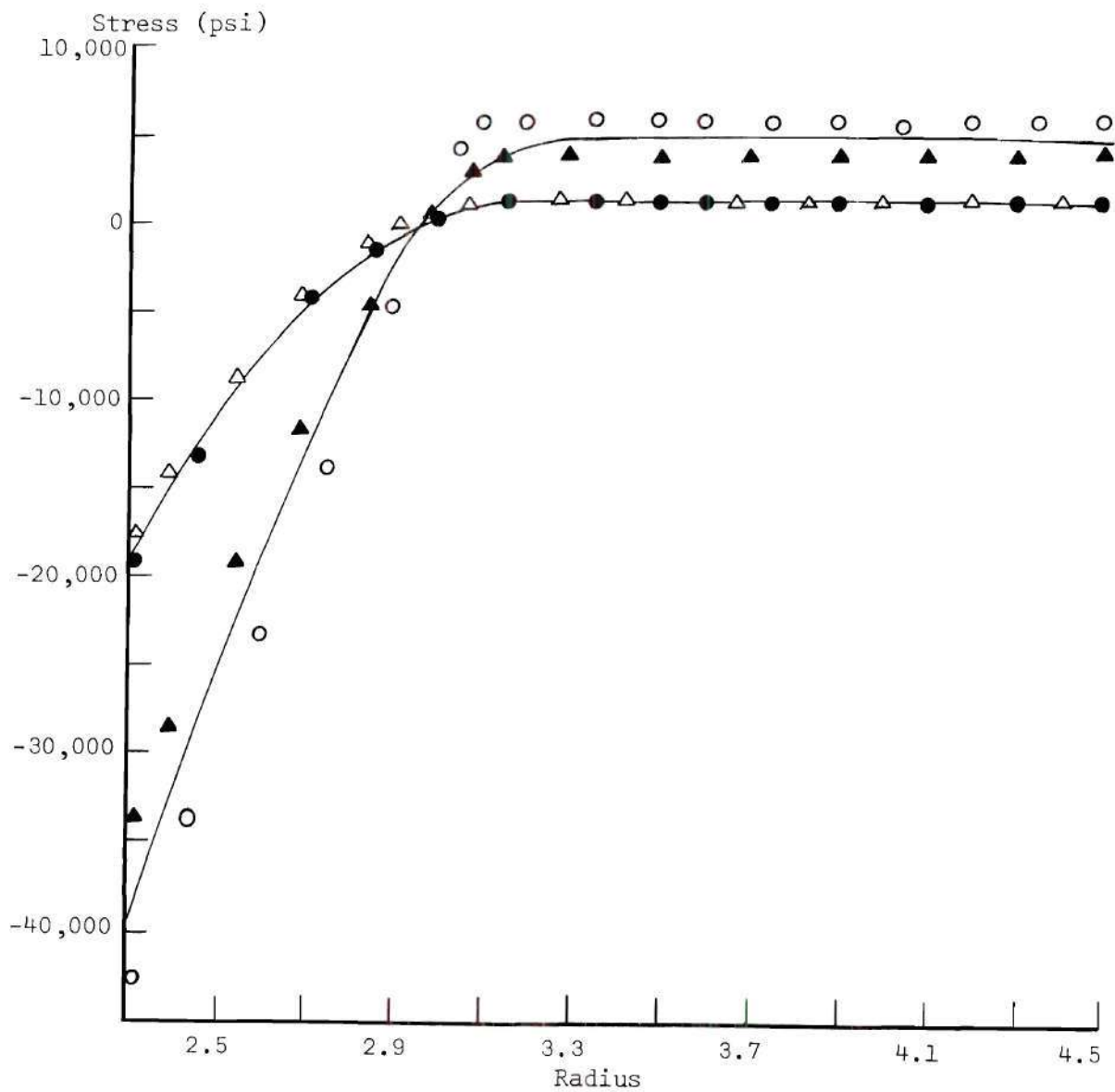
- Sachs Solution
- Coffin-MacGregor Solution
- △ Mendelson and Manson Solution

Figure 6. Residual Autofrettage Radial Stresses



- Sachs Solution
- Coffin-MacGregor Solution
- △ Mendelson and Manson Solution

Figure 7. Residual Autofrettage Tangential Stresses



- Sachs Closed End Solution
- Coffin-MacGregor Open End Solution
- △ Mendelson and Manson Open End Solution
- ▲ Mendelson and Manson Closed End Solution

Figure 8. Residual Autofrettage Axial Stresses

the cylinder due to the residual stresses the program will adjust the plastic deformation until a stress state is calculated in which there is no reyielding. Note that the residual stresses calculated by the Mendelson-Manson method differ very little with those calculated by the Sachs and the Coffin-MacGregor methods.

Machining

Before the forging is made into a gun, it is machined to the final dimensions shown by the dotted lines in Figure 1. This step takes place after the forging is autofrettaged.

For the muzzle section the bore radius was increased from 2.325 inches to 2.55 inches, and the outer diameter decreased from 4.5 inches to 3.75 inches. This removal of material will of course affect the residual stress distribution.

The effect of the machining can be calculated by considering a tube of the final bored and turned dimensions inside a tube of the original pre-machined dimensions. For example, in Table 4 note that the tube of dimension 2.55 inside radius and 3.75 outside radius, the radial stress is -41,104 psi at 2.55 inches, and -9053 psi at 3.75 inches. This is the equivalent of a tube of such dimensions with an internal pressure of 41,104 and an external pressure 9053 psi.

The elastic stresses to be removed can be calculated from standard theory of elasticity solutions. These elastic removal stresses are then subtracted from the action stresses to give the after-machining residual stress distribution.

The end load can be expressed as

$$\frac{Z}{2\pi r_p^2} = \int_{\frac{r}{r_p} = \frac{r_i^*}{r_p}}^{\frac{r}{r_p} = \frac{r_o^*}{r_p}} \sigma_z \left(\frac{r}{r_p} \right) d \left(\frac{r}{r_p} \right)$$

where * = the after-machined radius.

r_o = outside radius.

r_i = the inside radius.

r_p = the radius of the elastic-plastic interface.

This integral can be separated into an elastic part and a plastic part. The elastic part can be integrated. The equation with substitution in the plastic part can be written as:

$$\frac{Z}{2\pi r_p^2} = \frac{1}{2} \sigma_{zp} \left[\frac{(r_o^*)^2}{r_p^2} - 1 \right] + \int_{x = \ln \frac{r_i^*}{r_p}}^0 \sigma_z e^{2x} dx$$

where σ_{zp} is the value of the axial stress at the elastic-plastic interface.

The plastic part can be integrated numerically, perhaps by Simpson's rule. The end load removed by machining is then subtracted from the action axial stress to give the axial residual stress after machining.

Thermal Stresses

A computer program is used to calculate the thermal stresses. The program is based on the Mendelson and Manson iterative solution to the thermal stress problem. The program incorporates the strain distribution accompanying the autofrettage residual stresses, calculated by a different program, as input.

This strain distribution is considered the permanent deformation of the tube before the temperature is applied. Any further plastic deformation that accompanies the thermal stresses is superimposed on the permanent deformation and a total permanent deformation is calculated along with a stress distribution.

The program converges to a solution after nine iterations and there is little change after the second iteration. The program also accounts for any temperature dependency of the physical properties through a subroutine. In the subroutine the properties are tabulated and accessed as needed by the main program. The programs and subroutine are given in Appendix A.

Final Residual Stress Distribution

The final residual stress distribution is calculated by removing the temperature and calculating the stresses caused by the total permanent deformation of the cylinder. If at any point the combined stresses exceed the yield strength according to the von Mises condition, the total permanent deformation is adjusted and iteration continues. The final stress distribution is presented in Figures 9, 10 and 11.

Bore Diameter

Recall from Chapter II that the radial displacement, u , is related to the tangential strain, ϵ_θ , by the relationship

$$\epsilon_\theta = \frac{u}{r}$$

where r is the radius.

The diametral change of the bore, $2u$, can be calculated if the final tangential strain at the bore can be found. After machining, the strain accompanying the autofrettage residual stresses is -7.54451×10^{-4} at the bore. During thermal loading additional compressive stresses cause more compressive strain which brings the total tangential strain to -7.65735×10^{-4} at the bore. Some of the strain is elastic and some is plastic. Upon removal of the thermal loading, the elastic strain will be recovered. The recovered elastic strain is calculated from the final residual stresses by Hooke's Law and is

$$7.0220 \times 10^{-4}$$

Thus, the diametral change is $2\epsilon_\theta a$ which is $-.000335$ inches. This represents a decrease in bore diameter, although not of the magnitude reported in Table 1.

CHAPTER IV

EXPERIMENTAL RESULTS

A three-foot long section of the muzzle end of the five-inch naval gun was supplied M.I.T.; from a section of this, pure residual stresses were determined by the Sachs' boring out method. Initially, a piece 19 inches long was cut from this portion: this 19-inch piece was from the end furthest from the muzzle end.

Preliminary machine work consisted of squaring and facing the ends of this piece. It was then bored to a uniform internal diameter of 5.188 inches, thus giving a smooth instead of a rifled bore. The outer diameter was turned to insure that the inner and outer cylindrical surfaces were concentric. Six type A-1 SR4 wire resistance strain gages were mounted around the outer periphery of the tube at mid-length, at equal intervals of circumference. These gages were mounted in an axial direction and were electrically connected in series so as to obtain an average strain around the periphery of the gun section. An exactly similar arrangement was used for six more gages placed in a tangential direction around the periphery of the gun. Thus, two independent strain gage circuits were set up; a switching arrangement was set up so that only one decade resistance box and strain indicator would be required.

A special fixture was constructed so that the short tube could be attached to the face plate of a Monarch lathe. This fixture is the same as one described in reference (12).

When ready to begin machining, an initial zero reading of the two strain gage circuits was determined. Temperature was measured by a thermocouple attached directly to the gun section. The desired amount of material was then machined away from the bore of the tube. The tube was allowed to remain in its fixture overnight, and at approximately 8:00 a.m., further readings of strain and temperature were taken. This procedure was repeated until the tube was reduced to a thin shell. The purpose of the long rest period, approximately 20 hours, between machining operations and strain measurements was to allow thermal equilibrium to prevail. The variation of temperature observed was so small that it was not felt necessary to apply a temperature correction. The maximum variation from the temperature before the initial machining operation was 30°F (8).

By this method described above, residual strain data were obtained. The conversion of these strain measurements into residual stresses by the Sachs method will be illustrated by a step-by-step calculation procedure.

On the first page of Table 2 is shown the bore diameter before and after each machining operation. From these data the necessary quantities appearing in Equations (34), (35), and (36) can be calculated. These include the bore area F , $F_b - F$, $F_b + F$, $2F$, $F_b - F/2F$ and $F_b + F/2F$ where F_b is the cross sectional area of the original cylinder. On the rest of the first page of Table 2, the strain data ϵ_z and ϵ_t , as measured is indicated. These values of strain were plotted against the bore and F , and a smooth curve drawn through as

many of the data points as possible. The strain data were then graphically smoothed by means of the smooth curve, and the smoothed values of strain were rewritten in the sixth and seventh columns of page 1 of Table 2. Actually it was found that the experimental data plotted quite smoothly, and only very small corrections had to be applied.

Using the smoothed values of strain, the quantities Λ and θ were calculated as shown on the second page of Table 2. The quantities θ and Λ were then plotted against bore area, F , and smooth curves were drawn through the data points. In this case it was found that smooth curves could be drawn through all of the data points. If such had not been the case, it would have been necessary to add two more columns to Table 2 for smoothed values of θ and Λ . From the smoothed curves the necessary slopes $d\theta/dF$ and $d\Lambda/dF$ were then calculated by taking the slopes of tangents at the previously used values of F . Once the values of θ and Λ and their slopes have been arrived at, the residual stresses are computed from Equations (34), (35), and (36) as shown in the remainder of Table 2.

The final values of residual stress arrived at by this procedure for the muzzle piece are compared with the theoretical values of final residual stress in Figures 9, 10 and 11.

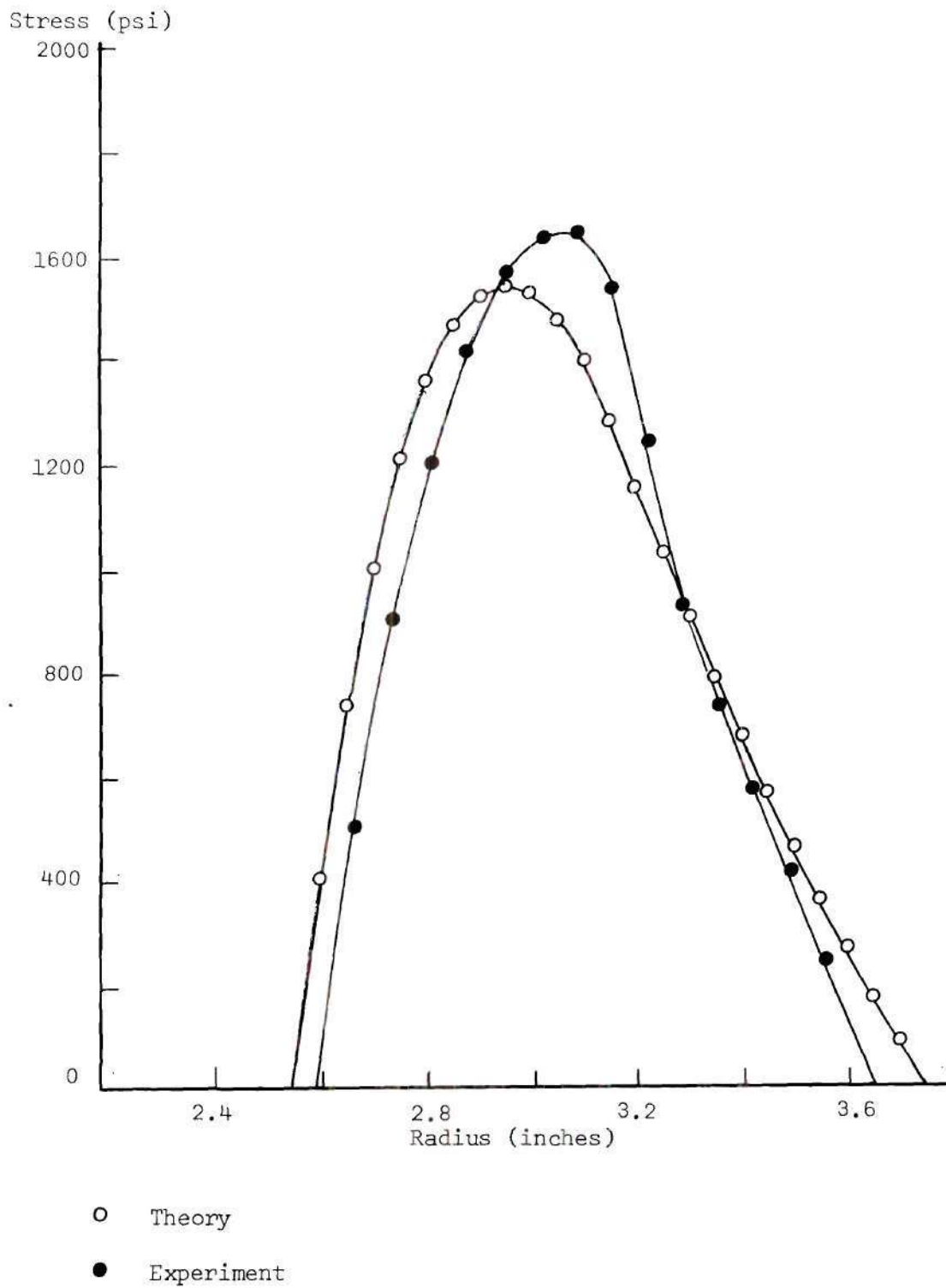
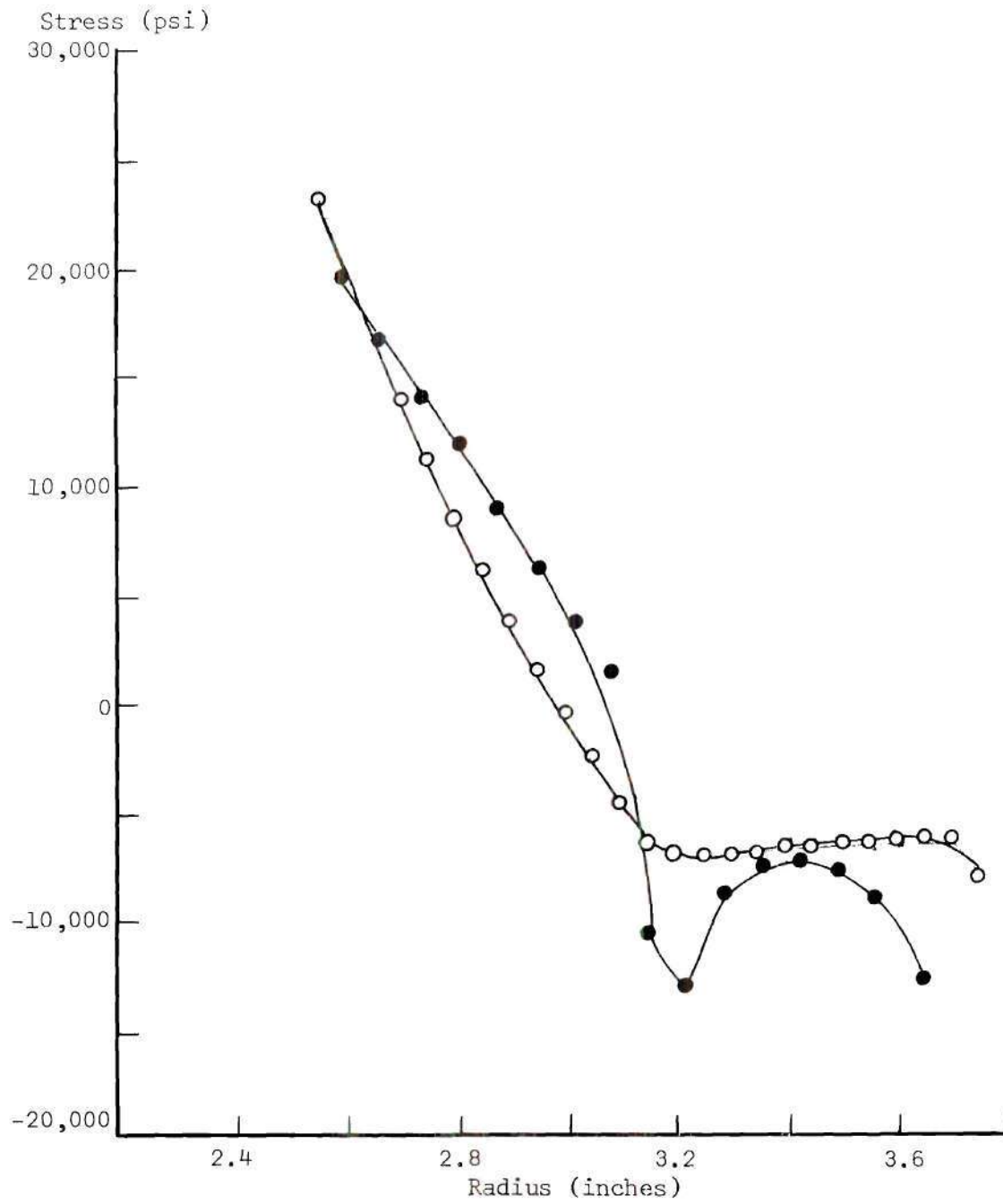
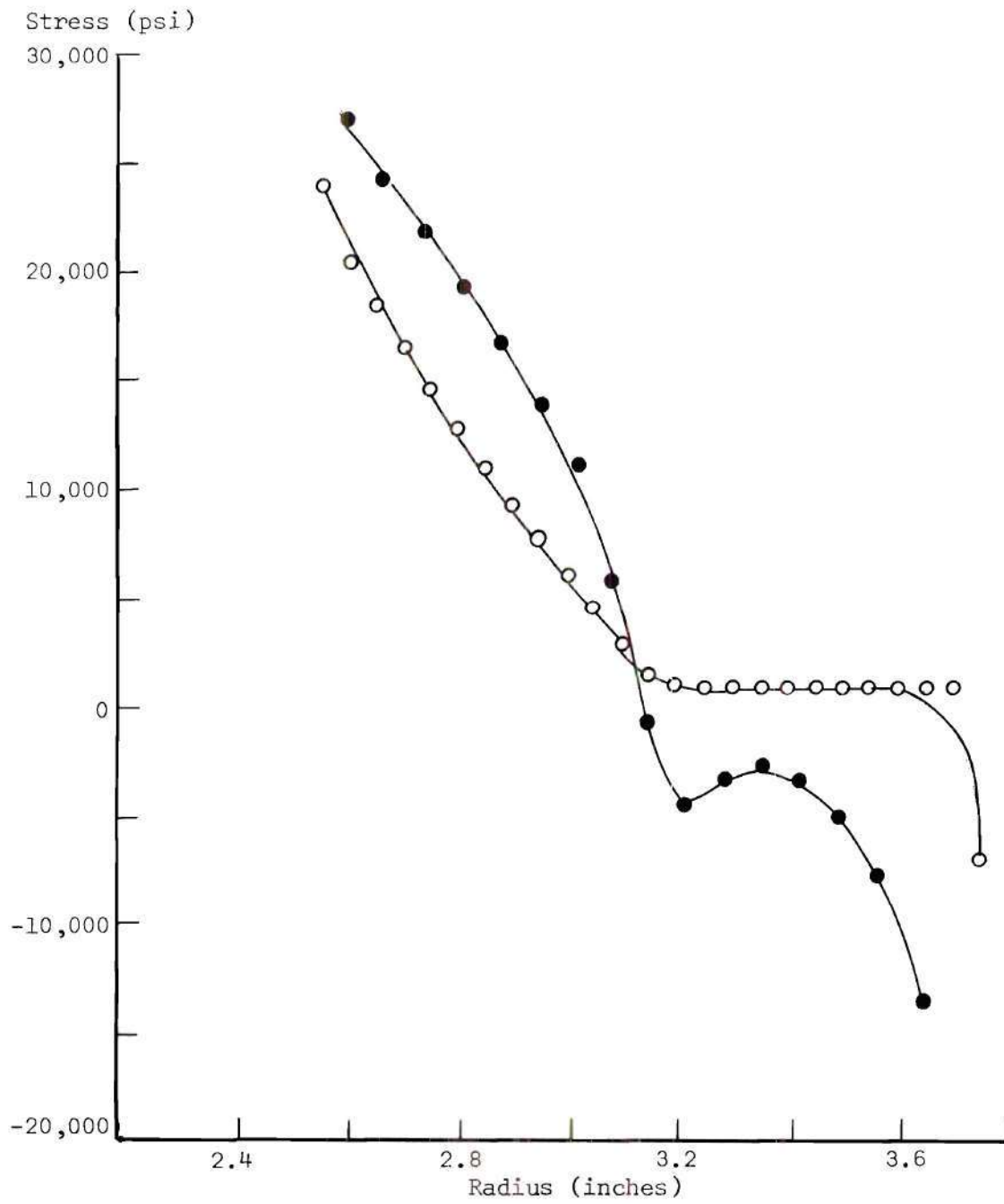


Figure 9. Final Residual Radial Stresses



- Theory
- Experiment

Figure 10. Final Residual Tangential Stresses



○ Theory

● Experiment

Figure 11. Final Residual Axial Stresses

CHAPTER V

DISCUSSION

The plots presented in Figures 9, 10 and 11 show the comparison of the final stress state after the cylinders are autofrettaged and then at some later date exposed to a temperature of 365°C at the bore (8). The curve labeled "experimental" is generated from the data supplied in reference (8).

The theoretical results were generated by the computer program which utilized the Mendelson and Manson method of determining thermal stresses. In Figure 9, the residual stress distribution in the radial direction, the agreement between theory and experiment is good, showing only slightly over 10% error in the worst case. For the tangential and axial stresses, the error is small from the bore to a radius of 3.1 inches for tangential and 3.15 for the axial residual stress.

From these points to the outer surface, there are differences. The shape of the experimental curve suggests that there is more plastic deformation in this region than accounted for by the theory. It appears that there is some plastic deformation from the outer surface, 3.75 inches back to a radius of 3.40 inches. The theory predicts plastic deformation only in a small region near the outer surface.

Note that due to the experimental procedure used there is no value reported for the residual stress at the bore. The first value of residual tangential stress given is at a radius of 2.594 inches

and for the tangential stress of 19,516 psi, which agrees very well with a theoretical stress of 19,424 psi at 2.6 inches. In the axial case, the first reported value is of 8604 psi at a radius of 2.594. The theoretical value of 6019 psi at 2.6 inches is not in such close agreement. This disagreement in the axial direction may arise from the fact that the gun is not strictly an open-end cylinder during thermal loading. Friction forces of the shell on the wall of the bore may induce further plastic deformation in that area. Pressure forces from the firing of the shell were also not considered.

The stresses arising from the firing pressure are from 10,000 to 50,000 psi, which are not negligible. The positive pressure inside would cause compressive radial stresses and tensile tangential and axial stresses. These stresses are opposite in direction from those of the autofrettage process already present and the thermal stresses generated during firing. The firing pressure stresses would have the effect of reducing the magnitude of the stresses on the cylinder. Thus, the predicted stresses, thermal and final residual, will be somewhat greater due to not considering the pressure effects of firing.

Disagreement possibly stems from the fact that the cylinder underwent several heat treatments before being autofrettaged and another heat treatment after the radial expansion. This final heat treatment definitely would affect the pattern of the autofrettage stresses. From the forging report, it is also obvious that the value of yield stress is not uniform throughout the casting. In the five transverse specimens tested, the yield strength ranged from 65,000 psi to 77,500 psi.

This could easily affect the amount of plastic deformation at various positions in the gun.

Recall that the heat is generated by the rapid fire condition which is not a steady state conduction problem. It was assumed that the problem was steady state to simplify the solution. It was also judged that this fluctuating temperature distribution could be approximated as a steady-state problem.

Transient temperature distributions would affect the material near the bore more than the rest of the material of the gun. Since in the area near the bore the theoretical solution agrees the best with the experimental data, it appears that the steady state analysis is sufficient to give an accurate thermal stress distribution.

Naturally, more refined results could be contained if more detailed information about the mechanical properties of the material were available.

It is concluded that this method of calculation gives a reliable estimate of the final interior diameter decrease, while providing an accurate picture of the final residual stress state in thick-walled cylinders.

Table 1. Bore Diameter Measurements Across Grooves Before and After 2245.62 Equivalent Service Rounds

Inches from Face of Breech	Diameter Across Grooves Before Proof Firing, Inches	Diameter Across Grooves After 2245.62 Esr., Inches	Expansion Across Grooves, Inches
218	5.101	5.101	-.006
223	5.101	5.096	-.005
228	5.101	5.096	-.005
233	5.101	5.096	-.005
238	5.101	5.096	-.005
243	5.101	5.097	-.004
248	5.101	5.097	-.004
253	5.101	5.097	-.004
258	5.101	5.098	-.003
263	5.101	5.098	-.003
268	5.101	5.098	-.003
273	5.101	5.098	-.003
278	5.101	5.098	-.003
283	5.101	5.098	-.003

Table 2. Calculation Procedure for Experimental
Residual Stresses Muzzle End Section

r	d	F	ϵ_z	ϵ_t	ϵ_z	ϵ_t
			Measured Microinches/Inch		Graphically Smoothed Microinches/Inch	
2.504	5.188	21.139	0	0	0	0
2.664	5.328	22.286	5	33	5	33
2.735	5.470	23.500	10	67	10	67
2.807	5.613	24.745	15	101	15	101
2.875	5.750	25.968	20	134	20	134
2.948	5.895	27.293	27	170	27	170
3.016	6.033	28.586	33	204	33	204
3.084	6.167	29.870	39	238	39	238
3.151	6.302	31.192	45	260	45	260
3.220	6.440	32.574	52	250	52	250
2.288	6.575	33.945	60	225	60	225
3.358	6.715	35.414	69	227	69	227
3.425	6.850	36.853	78	237	78	237
3.495	6.990	38.375	92	263	89	256
3.563	7.125	39.872	100	285	100	285
3.65	7.300	41.845			120	351

Table 2. Continued

Λ	θ	$\frac{d\Lambda}{dF}$	$\frac{d\theta}{dF}$	σr	$\sigma \theta$	σz
0	0	12.6	28.6	0	19,516	8604
14.9	34.5	12.6	28.6	499	16,780	7632
30.1	70.0	12.6	28.6	901	14,110	6633
45.3	105.5	12.6	28.6	1202	11,802	5614
60.2	140.1	12.6	28.6	1412	8,934	4615
78.0	178.1	12.6	28.6	1566	6,264	3478
94.2	213.9	12.6	28.6	1637	3,824	2407
110.4	249.7	10.0	28.6	1651	1,418	310
123.0	273.5	5.0	0	1541	-10,519	-2298
127.0	265.6	1.0	-10.3	1247	-13,121	-3880
127.5	243.0	3.5	0	932	-8,934	-3290
137.1	247.7	6.7	5.9	742	-7,648	-3099
149.0	260.4	9.5	11.0	583	-7,352	-3349
165.8	282.7	12.3	17.5	422	-7,747	-4055
185.5	315.0	15.2	26.2	258	-8,934	-5123
225.3	387.0	24.2	55.0	0	-12,758	-7427

Table 3. Elastic Thermal Stresses
Muzzle End Section

r	σ_r	σ_θ	σ_z
2.55	0	-72,007	-78,411
2.65	-2457	-58,294	-64,412
2.75	-4256	-45,489	-50,888
2.85	-5491	-33,462	-37,400
2.95	-6241	-21,840	-23,634
3.05	-6574	-10,944	-10,519
3.15	-549	-702	4,844
3.25	-6180	11,657	18,109
3.35	-5464	23,903	34,828
3.45	-445	35,467	47,409
3.55	-3167	46,246	62,691
3.65	-1675	56,320	74,257
3.75	0	65,900	85,511

Table 4. Action Autofrettage Stress
Muzzle End Section

r	σ_r	σ_θ	σ_z
2.325	-47,400	39,024	-9335
2.3401	-46,814	39,521	-8957
2.4601	-42,492	43,732	-6503
2.55	-41,104	45,055	-5712
2.5862	-38,190	47,806	-4047
2.7188	-33,895	51,576	-2143
2.8582	-29,646	55,529	-686
3.0047	-25,379	59,083	288
3.1588	-21,185	62,336	760
3.2	-20,114	61,266	760
3.35	-16,552	57,704	760
3.50	-13,457	54,589	760
3.60	-11,574	52,726	760
3.75	-9,053	50,205	760
3.90	-6,818	47,970	760
4.50	-4,826	45,978	760
4.20	-3,044	44,196	760
4.35	-1,443	42,596	760
4.50	0	41,152	760

APPENDIX A

THE MECHANICS OF THE COMPUTER SOLUTION

The program used to calculate the final residual stress state of a thick-walled cylinder was written in Fortran IV. The computer used is a UNIVAC 1108 owned and operated by the Rich Electronic Computer Center of the Georgia Institute of Technology. The Mendelson and Manson Thermal Stress solution was modified to calculate the autofrettage stresses by simply reducing the temperature to zero and using the autofrettage pressure as input. Inputs were of the free-field format with the data separated by commas. For the calculation of autofrettage residual stress, the input was: Number of Points, Outside Diameter, Pressure, Finite Difference Increment. The residual stresses were calculated by first using the Mendelson and Manson method of successive approximations to calculate the action stress distribution and the plastic strain distribution. Then the load was reduced to zero. Using the previously calculated values of plastic strain as first approximations of the strain (step 2 of the Mendelson and Manson method), the final stress and total residual strain distributions are calculated. In the muzzle section there was no re-yielding of the material so one iteration was all that was necessary to obtain convergence.

The residual stress distribution was compared with the Sachs and Coffin-MacGregor methods of residual stress calculation and was found to differ little from the residual stress distributions calculated by these

two methods. Figures 6, 7 and 8 show the residual stresses calculated by the three methods.

The solution for the thermal stresses is a bit more complex. The pressure, since the thermal loading occurred some time after the autofrettage process, is reduced to zero.

The total residual strain distribution calculated during the pressure solution is used as a first approximation of the plastic strains (step 2 of the Mendelson and Manson method). With this input, the solution requires eight iterations to converge to the action thermal stresses.

The temperature is reduced to zero, with the total plastic strain calculated during the action thermal stresses remaining the same. If any re-yielding occurs when the effective stress is greater than the yield strength, the total plastic strain is adjusted accordingly. If there is no re-yielding, one iteration is sufficient to obtain the residual stress distribution.

Variable Properties

A sub-program called PCON was written to account for variable properties. The data available for change of Young's modulus and coefficient of thermal expansion with temperature was in tabular form. Thus the sub-program PCON approximates the data as a series of steps. The sub-program calculates a value of Young's modulus and coefficient of thermal expansion for each station along the radius of the cylinder. As there were no data available for the temperature dependency of the

yield point of the gun steel, the yield point was assumed to be constant at 75,000 psi.

LITERATURE CITED

1. F. Kreith: "Principles of Heat Transfer," International Textbook Company (1967).
2. S. Timoshenko: "Strength of Materials, Part II," Van Nostrand (1956).
3. G. Sachs and O. Hoffman: "Introduction to the Theory of Plasticity for Engineers," McGraw-Hill Book Company (1953).
4. L. F. Coffin, Jr., C. W. MacGregor, J. C. Fisher, L. F. Lowrie, M. E. Graham: "The Stress Analysis and Design of Radially Expanded Guns," Report No. 2, Contract Nord 9107-Task F.
5. A. Mendelson and S. S. Manson, "Practical Solution of Plastic Deformation Problems in Elastic-Plastic Range," NACA Technical Note 4088, 1957.
6. D. F. Johnson: "Analysis of Elastic-Plastic Stress Distribution in Thin-Wall Cylinders and Spheres Subjected to Internal Pressure and Nuclear Radiation Heating," NASA Technical Note D-271, 1960.
7. G. Sachs and G. Espey, *The Iron Age*, Vol. 148, p. 63-71 (September 18, 1941) and p. 36-42 (September 25, 1941).
8. W. R. Clough and M. E. Shank: "A Study of Bore Construction in an Autofrettaged Gun," Navy Contract Nord 9107-TASR F.
9. British Iron and Steel Research Assoc.: "Physical Constants of Some Commercial Steels at Elevated Temperatures," Butterworths Scientific Publications, London, 1953.
10. F. W. Jones and J. Nortcliffe: "Note on the Temperature Variation of Young's Modulus of Various Steels," *Journal of the Iron and Steel Institute*, December, 1947, p. 535-536.
11. S. L. Hoyt: "Metal Data," p. 72, Rinehold Publishing Company, 1952.
12. W. R. Clough and M. E. Shank: "A Study of the Mechanical Behavior of Gun Steels and the Design of Loose Liner Guns." Navy Contract NAVORD 769, Project U, Part IV.